

## STUDY OF METHODS FOR PHASE CHARACTERIZATION IN INTERMETALLIC $UAl_x$

Giovanni Contubia, Rafael H. L. Garcia, Adonis M. Saliba-Silva, Elita F. Urano de Carvalho, and Michelangelo Durazzo

<sup>1</sup> Instituto de Pesquisas Energéticas e Nucleares (IPEN / CNEN - SP)  
Av. Professor Lineu Prestes 2242  
05508-000 São Paulo, SP  
[gconturbia@ipen.br](mailto:gconturbia@ipen.br)

### ABSTRACT

The  $UAl_x$  is an intermetallic compound used in the manufacture of irradiation targets for molybdenum-99 production. The fissionable uranium-235 is presented in the form of intermetallic  $UAl_x$  powder, which is dispersed in an aluminum matrix. This paper aims at studying methods for phase characterization of the intermetallic. The index  $x$  identifies the phase composition of the compound, usually a mixture of  $UAl_2$ ,  $UAl_3$  and  $UAl_4$ . The phase composition was quantified in the  $UAl_x$  powder and  $UAl_x$ -Al dispersion by means of image analysis and x-ray diffraction, applying the Rietveld method. Both methods allowed the quantification of the presented phases. The results from the two methods differed from each other with respect to the concentration determination. Possible error sources are discussed in this paper. The quantification method based on x-ray diffraction showed potential to be applied to the RMB Project for phase quantification in  $UAl_x$ -Al dispersion targets, which is required by specification.

### 1. INTRODUCTION

Every year the world demands more than 30 million medical imaging procedures that use technetium-99m radioisotope ( $Tc^{99m}$ ), which correspond to approximately 80% of all nuclear medicine diagnoses. [1] This radiopharmaceutical product derives from the radioactive decay of molybdenum-99 ( $Mo^{99}$ ), which is commercially produced in research reactors by irradiation targets that contain uranium-235. However, continuous supplying of  $Mo^{99}$  has decreased over the last decade, mainly due to shutdowns that have occurred in the main research reactors that produce radioisotopes [2]. To deal with this scenario, Brazil has decided to build up a multipurpose reactor which among other functions will irradiate uranium targets to produce enough  $Mo^{99}$  to meet domestic demand.

There are currently two technologies available to produce uranium targets. One is based on metallic uranium thin foils [3] and the other one is based on a uranium-aluminum alloy dispersed in an aluminum matrix [4].

The binary system, uranium and aluminum, forms a phase diagram which shows the existence of intermetallic compounds consisting of three phases,  $UAl_2$ ,  $UAl_3$  and  $UAl_4$ . The mixture of these phases is known in the literature as  $UAl_x$  [5]. Because of its experience acquired over the years in the manufacturing technology based on dispersion fuels, IPEN has decided to adopt this technology for fabricating  $UAl_x$ -Al dispersion targets for future  $Mo^{99}$  production in Brazil.

Characterizing the phase composition in  $UAl_x$  powder used as raw material for target fabrication is important because the maximum uranium concentration depends on the phase composition presented in the starting powder. Furthermore, it is important to mention that the  $UAl_3$  and  $UAl_4$  are more easily dissolved in alkaline solutions than the  $UAl_2$ , which defines, ultimately, the radiochemical processing throughput after the irradiation [6]. So, the presence of  $UAl_2$  in the  $UAl_x$ -Al dispersions target also must be quantified.

This paper aims at investigating methods to quantify the phases present in  $UAl_x$  powder and  $UAl_x$ -Al dispersions. Two possible methods were investigated: image analysis and x-ray diffraction.

## 2. MATERIALS AND METHODS

The intermetallic was prepared from a mixture of metallic uranium and metallic aluminum metal in stoichiometric proportions to obtain  $UAl_2$  (81.5 wt% U). The starting materials were charged into a zirconium crucible and melted using a 15 kW induction furnace. Prior the melting, the furnace was purged with argon after vacuum of  $2.6 \times 10^{-3}$  mbar. The  $UAl_x$  ingot was ground in a mortar under argon atmosphere.

A mixture of aluminum and  $UAl_x$  powders corresponding to 50 and 45 vol% respectively has been pressed to form the target meet, which is called briquette. It contains  $UAl_x$  particles dispersed in an aluminum matrix. The particle size distribution of the  $UAl_x$  powder in the briquette was 80 wt% of 44 to 150  $\mu$ m particles and 20 wt% of particles smaller than 44  $\mu$ m.

The roll billet consists of a picture frame, two cover and a briquette. This components were assembled and joined by Tungsten Inert Gas (TIG) welding and then rolled to form the targets, according to the picture-frame technique [7-9]. Prior the rolling operation, the briquettes were degassed at 250 °C for 3 hours under vacuum of  $0.8 \times 10^{-3}$  mbar. The assemblies were hot-rolled at 450 °C in four rolling passes. The final specified thickness for the target was reached with two cold-rolling passes. Table 1 shows the typical rolling scheme adopted to manufacture  $UAl_x$ -Al dispersion targets.

**Table 1: Typical rolling scheme to manufacture  $UAl_x$ -Al dispersions targets**

Target Number	Thickness (mm) (assembly starting thickness= 9.23 mm)					
	P1 (hot)	P2 (hot)	P3 (hot)	P4 (hot)	P5 (cold)	P6 (cold)
1	5.90	→ withdrawn for analysis (WA)				
2	5.98	3.91	→ WA			
3	6.03	3.90	2.66	→ WA		
4	6.00	3.90	2.65	1.77	→ WA	
5	6.02	3.89	2.64	1.77	1.63	→ WA
6	5.99	3.90	2.64	1.75	1.64	1.52

P = rolling pass

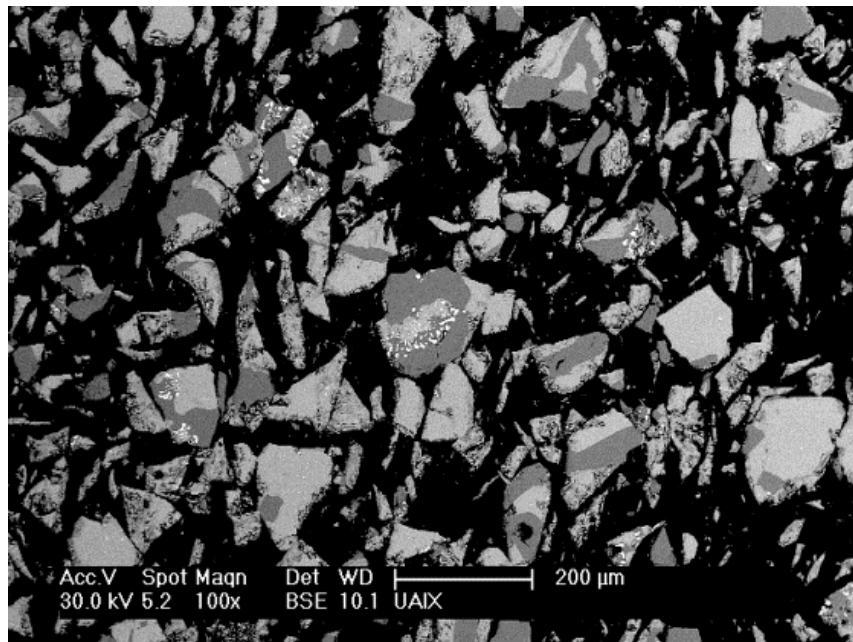
X-ray diffraction data were collected from samples of polished briquettes and rolled target meats by a Rigaku Multiflex diffractometer, operating with Cu-K $\alpha$  radiation at 40 kV and 20 mA, with a scan of 0.02° and for 8 s counts. The reference information was obtained from the

ICDD files 58195, 58196 and 24233. The crystalline phases were quantified using the Rietveld method with GSAS for data refinement.

The phase composition was also quantified by studying the microstructure of briquettes and rolled meats through scanning electron microscopy (backscattered electron image) and energy dispersive spectroscopy. A Philips XL30 microscope was used. Image analysis was used for quantifying the phases by using the software Omnimet Enterprise Buehler.

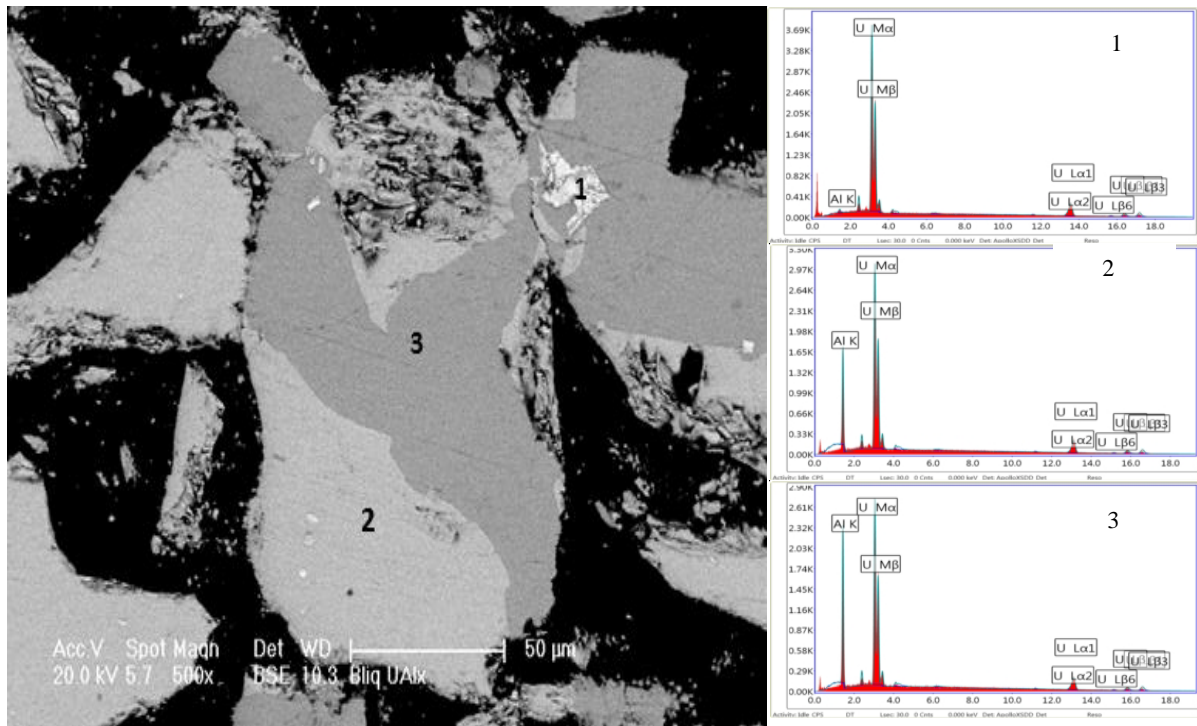
### 3. RESULTS AND DISCUSSION

Fig. 1 shows a scanning electron micrograph of the cross section of a  $UAl_x$ -Al briquette, where the  $UAl_x$  particles are homogeneously dispersed in the aluminum matrix. Because of the atomic number contrast obtained from the backscattered electrons, which is sensitive to the composition, it was possible to observe three shades of gray, which indicate the existence of three phases.



**Figure 1: Scanning electron micrograph from a  $UAl_x$ -Al briquette cross-section illustrating the dispersion and the phases presented (backscattered electrons).**

EDS analysis (Fig. 2) were used to quantify the levels of uranium and aluminum in the three phases. Region 1 (lighter gray tone, almost white) showed a composition of 99.0 wt% U and 1.0 wt% Al. As discussed later, this phase was identified by X-ray diffraction as UO. The grayscale observed on region 2 corresponded to the concentration of 82.5 wt% uranium and 17.5 wt% aluminium, while the darker gray tone related to the region 3 showed a composition of 76.6 wt% U and 23.4 wt% Al. Based on the stoichiometric composition, the compositions of the regions 2 and 3 characterize the  $UAl_2$  and  $UAl_3$ , respectively



**Figure 2: Scanning electron micrograph and EDS analysis of the regions designated by 1, 2 and 3. The compositions of regions 2 and 3 indicate the presence of  $UAl_2$  and  $UAl_3$ , respectively (backscattered electrons).**

The volumetric fractions of the three phases present were determined by using image analysis. Eight images were analyzed. Fig. 3 shows a typical image that was analyzed. The cyan color (light blue) was used to identify the  $UAl_2$  phase, the yellow color was used to identify the  $UAl_3$  phase and the dark blue color was used to identify the denser phase of  $UO_2$ . The red color was used to identify the aluminum matrix.

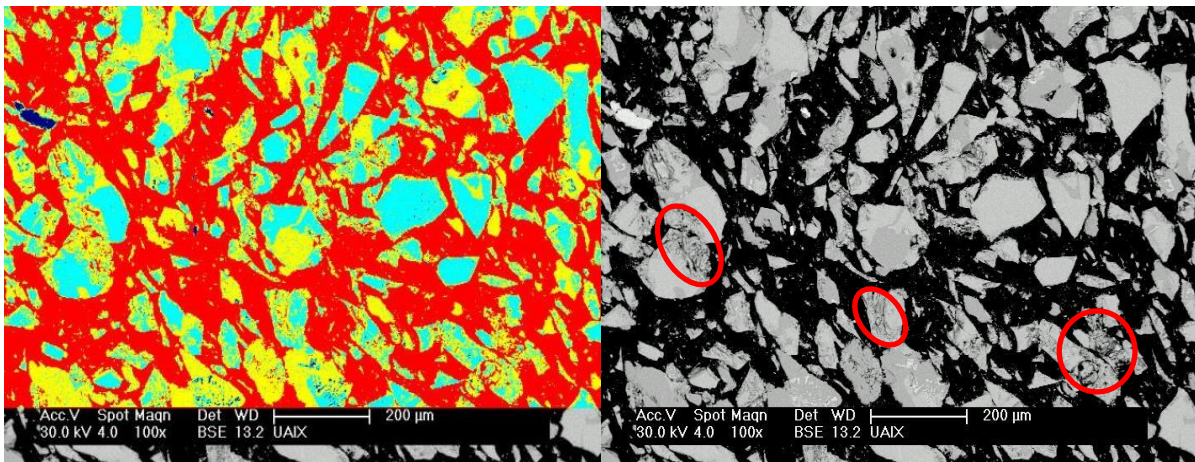


**Figure 3: Left, image processed by the image analyze. Right, unprocessed image.**

The red circles in Fig.3 (right) illustrate regions where fragmentation of  $UAl_2$  (fragile phase) can be observed. The fragments of fragmented  $UAl_2$  particles present a dark shade of gray that is confused with the shade of gray of  $UAl_3$  particles. This is an important source of error, as discussed below.

The phase quantitation by image analysis resulted in 42.6 wt% for  $UAl_2$ , 56.26 wt% for  $UAl_3$  and 1.2 wt% for  $UO$ . Chemical analysis determined the uranium content in the powder as 80.74 wt%, with a uranium loss of 0.76 wt% compared to the nominal uranium content of the starting composition of the charge of fusion (81.50 wt%). This loss can be attributed to the oxidation of uranium alloy during the melting process to form  $UO$ .

Considering that the uranium content was determined by chemical analysis and neglecting the presence of the oxidized phase remaining in the sample, from the U-Al equilibrium diagram [5] the expected phase composition in the powder would be about 89.4 wt% for the  $UAl_2$  and 10.6 wt% for  $UAl_3$ . The composition resulted from the image analysis shows underestimated values for the  $UAl_2$  concentration. This result can be explained by the fragmentation of the fragile  $UAl_2$  particles, which occurs when pressing and rolling the  $UAl_x$ -Al dispersion. Differences in height (porosity) in the regions of fragmentation cause fewer backscattered electrons reaching the detector, which decrease the brightness in these regions and result in a darker shade of gray on the edges of the  $UAl_2$  particles and fragments thereof. This darker shade of gray in the image is confused by the image analyzer as  $UAl_3$ , as illustrated by the regions marked with red circles in Fig 3. The image analyzer distinguishes the edges of the  $UAl_2$  particles and its fragments as  $UAl_3$ . Thus, the processed image leads to a concentration underestimated for the  $UAl_2$  fraction and overestimated for the  $UAl_3$  fraction. This effect does not occur with the  $UAl_3$  particles due to its greater ductility [7].

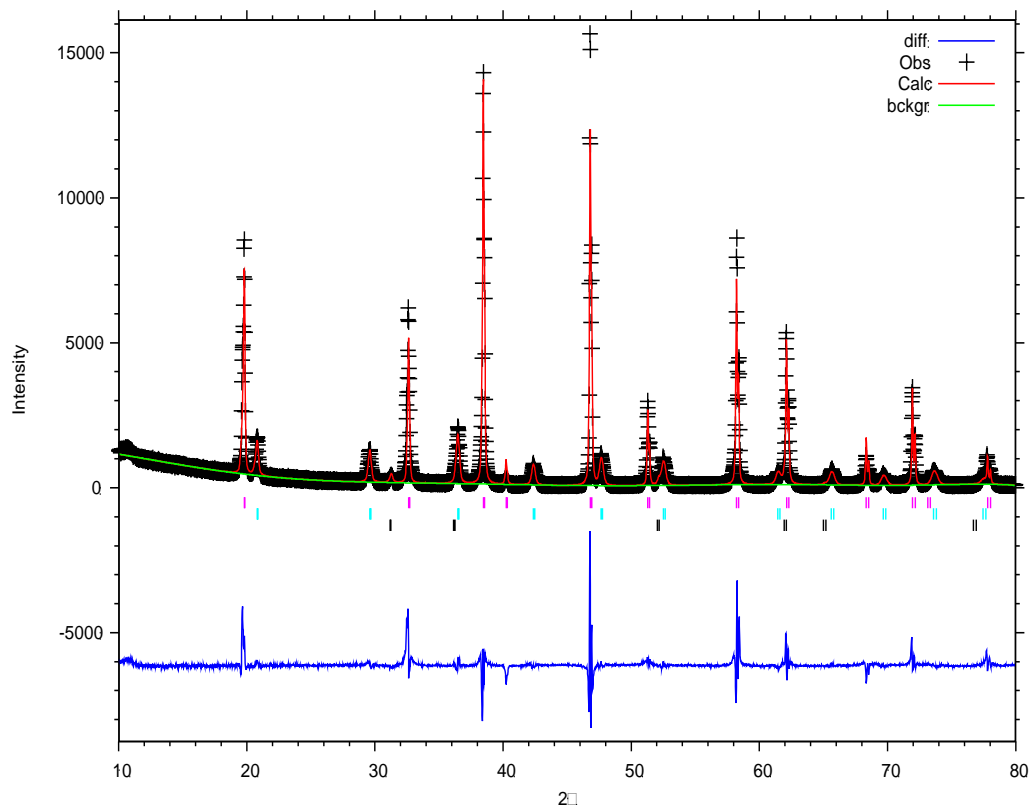


**Figure 4: Experimental and calculated diffractograms for the  $UAl_x$  powder. The peaks marked with purple bars are from  $UAl_2$ , cyan bars from  $UAl_3$  and black bars from  $UO$ .**

The phase composition obtained by X-ray diffraction for the same  $UAl_x$ -Al briquette analyzed by image analysis is presented in Fig. 4, which shows the experimental and

calculated diffraction pattern by Rietveld method. The value of  $\chi^2$  resulting from the simulation was 66, showing a reasonable agreement between the experimental and the theoretical values.

As mentioned before, the compositional analysis of the phases obtained by SEM-EDS indicated the existence of  $UAl_2$ ,  $UAl_3$  and a third phase rich in uranium (lighter gray tone, almost white, region 1 in Fig. 2). This observation was confirmed by X-ray diffraction, which shows that the uranium-rich phase is UO. The results for the phase measurement from the Rietveld method showed 85.4 wt% for  $UAl_2$ , 11.4 wt% for  $UAl_3$  and 3.2 wt% for UO.

By Analyzing the results, it can be observed that they who? are extremely different with respect to the phase quantification. Table 2 summarizes the results obtained by image analysis and X-ray diffraction with Rietveld refinement.

**Table 2: Results for phase quantitation in  $UAl_x$  powder (wt%)**

Phase	Rietveld	Image Analysis	Expected Composition (chemical analysis)
$UAl_2$	85.4	42.6	89.4
$UAl_3$	11.4	56.2	10.6
UO	3.2	1.2	0

The  $UAl_2$  content determined from Rietveld refinement is below the one expected according to the chemical analysis. This indicates low fit between the experimental and calculated data by the method, which could be attributed to the impossibility of rotating the sample during the X-ray diffraction analysis, since it was not possible to use the "spinner" during the analysis to avoid preferred orientation. Anyway, the approximation can be considered good, with a deviation of around 5 %.

In order to verify the feasibility of the method for following the phase composition during the  $UAl_x$ -Al dispersion target manufacturing process, core samples were analyzed by the x-ray diffraction with Rietveld refinement after each rolling pass, as showed in Table 1. The aim was to follow the phase composition evolution during the rolling process for target fabrication. This aspect is important, since the maximum  $UAl_2$  phase concentration presented in the target must be determined by specification request. Polished specimens of the targets meat were analyzed by X-ray diffraction applying Rietveld refinement. The results are presented in Table 3.

Fig. 5 presents the phase composition evolution inside the target meat during the target manufacturing process. After the first hot-rolling pass it occurs remarkable transformation of  $UAl_2$  to  $UAl_3$  due to the solid state reaction with aluminum from the dispersion matrix. This reaction results from the heat treatment performed before the first hot-rolling (1 hour at 450 °C). In the subsequent hot-rolling passes does not occurs significant transformation, keeping the composition stable, within the error of the Rietveld method. After the last hot-rolling pass a new thermal treatment is accomplished with duration of 1 hour at 450 °C (blister test). The objective of this new heat treatment is to verify the bonding quality. After this new heat treatment, a significant transformation from  $UAl_2$  to  $UAl_3$  and the starting  $UAl_4$  formation occur again, which is formed by the reaction of  $UAl_3$  with the aluminum matrix of the dispersion. The oxide concentration keeps unchanged within the error of the method.

**Table 3: Results for phase quantitation in  $UAl_x$  target meats (wt%)**

Rolling Pass	$UAl_2$	$UAl_3$	$UAl_4$	UO
Briquette	85.4	11.4	0	3.2
P1 (hot)	74.3	24.3	0	1.4
P2 (hot)	71.7	27.2	0	1.1
P3 (hot)	75.5	22.7	0	1.8
P4 (hot)	73.1	24.7	0	2.2
P5 (cold)	47.6	47.1	4.6	0.7
P6 (cold)	48.1	45.6	5.3	1.0

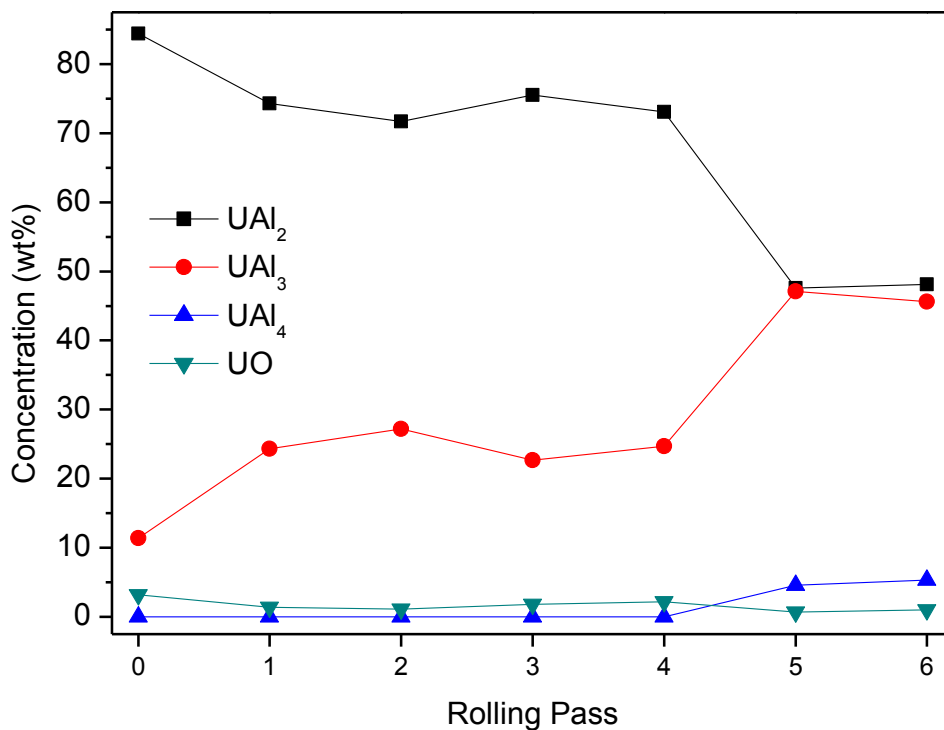


**Figure 5: Phase composition evolution during the target manufacturing process.**

### 3. CONCLUSIONS

Two possible methods for phase quantification in dispersion based  $UAl_x$ -Al irradiation targets were successfully studied.

The method based on scanning electron microscopy and image analysis proved to be inapplicable due to some errors related to the fragmentation of  $UAl_2$  particles.

The method based on X-ray diffraction with Rietveld refinement proved to be applicable, with an estimated error of 5 %. By applying this method, it was possible to follow the

evolution of the phase composition during the target manufacturing process. However, additional work on these methods is necessary to determine the error of the method.

## ACKNOWLEDGMENTS

The authors are grateful to FAPESP and CNPq for the research grants (2011/13849-9 and 471008/2011-7) provided for this work.

## REFERENCES

1. "A Supply and Demand Update of the Molybdenum-99 Market-2012," <http://www.oecd-nea.org/med-radio/#docs> (2012).
2. "The Supply of Medical Radioisotopes: the Path to Reliability," <http://www.oecd-nea.org/med-radio/#docs> (2011).
3. Briyatmoko, B.; Guswardani, B.; Purwanta, S.; Permania, S.; Basiran, D.; Kartaman, M. "Indonesia's current status for conversion of Mo-99 production to LEU fission," *Proceeding of International Meeting on Reduced Enrichment for Research and Test Reactors*, Prague, Czech Republic, September 23–27, 2007. [http://www.rertr.anl.gov/RERTR29/Abstracts/S6-1\\_Briyatmoko.html](http://www.rertr.anl.gov/RERTR29/Abstracts/S6-1_Briyatmoko.html)
4. Kohut, C.; Fuente, M.; Echenique, P.; Podesta, D.; Adelfang, P. "Targets development of low enrichment for production of Mo99 for fission," *Proceeding of International Meeting on Reduced Enrichment for Research and Test Reactors*, Las Vegas, Nevada, October 1-6, 2000. <http://www.rertr.anl.gov/Web2000/Title-Name-Abstract/Fuente00.html>
5. Bramfitt, B. L.; Leighly H. P. Jr. "A Metallographic Study of Solidification and Segregation in Cast Aluminum-Uranium Alloys," *Metallography*, **I**, pp. 165-193 (1968).
6. Cols, H. J.; Cristini, P. R.; Manzini, A. C. "Mo – 99 from low-enriched uranium," *Proceeding of International Meeting on Reduced Enrichment for Research and Test Reactors*, Las Vegas, Nevada, October 1-6, 2000. <http://www.rertr.anl.gov/Web2000/Title-Name-Abstract/Cristi00.html>
7. Cunningham, J. E.; Boyle, E. J. "MTR-Type fuel elements," *Proceeding of the International Conference on Peaceful Uses of Atomic Energy*, Geneva, 8-20 August. 1955. Vol. 9: Reactor technology and chemical processing, pp.203-207 (1956).
8. Durazzo, M.; Urano de Carvalho, E. F.; Saliba Silva, A. M.; Souza, J. A. B.; Riella, H. G. "Current status of U<sub>3</sub>Si<sub>2</sub> fuel elements fabrication in Brazil," *Proceeding of International Meeting on Reduced Enrichment for Research and Test Reactors*, Prague, Czech Republic, September 23–27, 2007. [http://www.rertr.anl.gov/RERTR29/Abstracts/S11-8\\_Durazzo.html](http://www.rertr.anl.gov/RERTR29/Abstracts/S11-8_Durazzo.html)
9. Durazzo, M.; Urano de Carvalho, E. F.; Saliba Silva, A. M.; Souza, J. A. B.; Riella, H. G. "Fabricação de elementos combustíveis a base de U<sub>3</sub>Si<sub>2</sub> no Brasil," *Rev. Bras.Pesq.Des.*, **Vol. 9, n. 1**, pp.18-26 (2007).